fit between the observed and calculated frequencies for all molecules. The trial force constants were refined to reproduce the observed $C^{16}O$ and $C^{18}O$ vibrations to within an average of 0.8 cm^{-1}. Data typical of that obtained are provided in Table II for the various isotopic species of $W(CO)_5P(OCH_2)_3Et$.

^{13}C NMR Measurements. The ^{13}C NMR spectra were recorded on a JEOL FX60 operated at 15.03 MHz with an internal deuterium lock. Samples were run in $CDCl_3$ solvent in 10-mm tubes. Spectra for determining the oxygen-18 shifted ^{13}C resonances resulted from the accumulation of 14 000 transients employing a sweep width of 500 Hz (16K data block) with an acquisition time of 16.4 s, a pulse repetition rate of 17.0 s, and a flip angle of 90°.

Acknowledgments. The financial support of this research by the National Science Foundation through Grant CHE 78-01758 is greatly appreciated.

Synthesis and Electronic and Redox Properties of "Double-Cubane" Cluster Complexes Containing $MoFe_3S_4$ and WFe_3S_4 Cores

Thomas E. Wolff,[1a] Philip P. Power,[1a] Richard B. Frankel,[1b] and R. H. Holm*[1a]

Contribution from the Department of Chemistry, Stanford University, Stanford, California 94305, and the Francis Bitter National Magnet Laboratory, Massachusetts Institute of Technology, Cambridge, Massachusetts 02139. *Received January 21, 1980*

Abstract: The reaction system $MS_4^{2-}/3\text{-}3.5FeCl_3/9\text{-}12NaSR$ (M = Mo, W) in methanol or ethanol affords as principal products four "double-cubane" cluster anions, $[M_2Fe_6S_9(SR)_8]^{3-}$ (**1**), $[Mo_2Fe_6S_8(SR)_9]^{3-}$ (**2**), $[M_2Fe_7S_8(SR)_{12}]^{3-}$ (**3**), and $[M_2Fe_7S_8(SR)_{12}]^{4-}$ (**4**), which are isolable as appropriate quaternary ammonium salts. Syntheses of cluster types **1** (M = W), **3**, and **4** are described together with spectroscopic and voltammetric properties of the four cluster types. All clusters exhibit isotropically shifted ^1H NMR spectra which serve as criteria for adequate purity, reveal from shift patterns contact and dipolar mechanisms at terminal and bridge substituents, respectively, and support the existence of single geometrical isomers in solution. Cluster types **1** and **2** form three-membered electron-transfer series in which individual $MFe_3S_4(SR)_3$ clusters are reduced in weakly coupled steps. Cluster type **3** affords a four-membered series in which the initial reduction is $Fe^{III} \rightarrow Fe^{II}$ in the $Fe(SR)_6$ bridge unit and subsequent reductions occur at individual clusters. Potential separations for the latter two steps (~0.10 V) more closely approach the statistical value of 36 mV than do those of types **1** and **2** (~0.19 V), owing to larger intercluster separations. The presence of Fe^{III} and Fe^{II} in the bridge units of type **3** and **4** clusters, respectively, is demonstrated by Mössbauer spectroscopy. From observations of narrow intervals of ^{57}Fe isomer shifts, hyperfine magnetic fields at Fe sites, terminal methylene proton contact shifts, and redox potentials of **1** and **2** it is concluded that the Fe_3 portions of MFe_3S_4 core units are electronically delocalized and, within and among all cluster types **1**–**4**, are virtually equivalent electronically. Core Fe isomer shifts are considered to accord best with the mean oxidation state $Fe^{2.67+}$. This conclusion, together with prior observations of a pronounced structural core similarity in all clusters, leads to the core formal electronic descriptions $[Mo^{4+}Fe^{3+}{}_2Fe^{2+}S_4]^{4+} + [Mo^{3+}Fe^{3+}{}_2Fe^{2+}S_4]^{3+}$ (type **1**) and $2[Mo^{3+}Fe^{3+}{}_2Fe^{2+}S_4]^{3+}$ (types **2**–**4**), thereby defining total oxidation levels of the cores in each cluster type. Full tabulations of Mössbauer spectral parameters and ^1H NMR isotropic shifts are presented together with representative Mössbauer and NMR spectra and cyclic voltammograms.

Introduction

The burgeoning interest in iron–molybdenum–sulfur complexes and their tungsten counterparts arises in large measure from recent spectroscopic studies[2-5] of the FeMo proteins of nitrogenase and the FeMo cofactor obtainable therefrom. The results of these investigations point to the existence of an Fe–Mo–S cluster as yet incompletely defined in terms of composition and structure and not encountered in any other biological system or as a product of chemical synthesis. Several laboratories are engaged in the synthesis of Fe–Mo–S cluster complexes in order to generate species of possible relevance to the biological cluster. To date, synthetic methods productive of Fe–Mo–S clusters have utilized as starting materials the tetrathiometalates MS_4^{2-} (M = Mo, W).[6] The general tendency of these ions to form heterometallic complexes via sulfide bridging has been demonstrated in other contexts,[6,7] especially by the research of Müller and co-workers.[6,7a]

The classes of Fe–M–S clusters (M = Mo, W) derived from tetrathiometalates are most simply organized in terms of cluster nuclearity: binuclear, $[(PhS)_2FeMS_4]^{2-}$,[8] $[Cl_2FeMS_4]^{2-}$,[9] $[S_5FeMS_4]^{2-}$;[8b] trinuclear, $[Fe(MS_4)_2]^{2-}$,[10] $[Fe(NO)(MS_4)_2]^{2-}$,[10]

---

[1] (a) Stanford University; (b) Francis Bitter National Magnet Laboratory.

[2] S. P. Cramer, K. O. Hodgson, W. O. Gillum, and L. E. Mortenson, *J. Am. Chem. Soc.*, **100**, 3398 (1978).

[3] S. P. Cramer, W. O. Gillum, K. O. Hodgson, L. E. Mortenson, E. I. Stiefel, J. R. Chisnell, W. J. Brill, and V. K. Shah, *J. Am. Chem. Soc.*, **100**, 3814 (1978).

[4] J. Rawlings, V. K. Shah, J. R. Chisnell, W. J. Brill, R. Zimmerman, E. Münck, and W. H. Orme-Johnson, *J. Biol. Chem.*, **253**, 1001 (1978).

[5] B. H. Huynh, E. Münck, and W. H. Orme-Johnson, *Biochim. Biophys. Acta*, **527**, 192 (1979).

[6] E. Diemann and A. Müller, *Coord. Chem. Rev.*, **10**, 79 (1973).

[7] For recent examples cf.; (a) A. Müller, H. Bögge, E. Königer-Ahlborn, and W. Hellmann, *Inorg. Chem.*, **18**, 2301 (1979); A. Müller, H. Bögge, and E. Königer-Ahlborn, *J. Chem. Soc., Chem. Commun.*, 739 (1978); A. Müller, H. Dornfeld, G. Henkel, B. Krebs, and M. P. A. Viegers, *Angew. Chem., Int. Ed. Engl.*, **17**, 52 (1978); A. Müller, T. K. Hwang, and H. Bögge, *ibid.*, **18**, 628 (1979); A. Müller, I. Paulat-Böschen, B. Krebs, and H. Dornfeld, *ibid.*, **15**, 633 (1976); (b) J. C. Huffman, R. S. Roth, and A. R. Siedle, *J. Am. Chem. Soc.*, **98**, 4340 (1976); J. K. Stalick, A. R. Siedle, A. D. Mighell, and C. R. Hubbard, *ibid.*, **101**, 2903 (1979).

[8] (a) D. Coucouvanis, E. D. Simhon, D. Swenson, and N. C. Baenziger, *J. Chem. Soc., Chem. Commun.*, 361 (1979); (b) D. Coucouvanis, N. C. Baenziger, E. D. Simhon, P. Stremple, D. Swenson, A. Kostikas, A. Simopoulos, V. Pêtrouleas, and V. Papaefthymiou, *J. Am. Chem. Soc.*, **102**, 1732 (1980).

[9] (a) D. Coucouvanis, N. C. Baenziger, E. D. Simhon, P. Stremple, D. Swenson, A. Simopoulos, A. Kostikas, V. Pêtrouleas, and V. Papaefthymiou, *J. Am. Chem. Soc.*, **102**, 1730 (1980); (b) P. P. Power and R. H. Holm, unpublished results.

0002-7863/80/1502-4694$01.00/0

$[\mathrm{Cl_2FeMoS_4FeCl_2}]^{2-}$;[8a] tetranuclear, containing two $\mathrm{MFe_3S_4}$ cubane-type core units, $[\mathrm{M_2Fe_6S_9(SR)_8}]^{3-}$[11-13] (**1**), $[\mathrm{M_2Fe_6S_8(SR)_9}]^{3-}$[12,14-16] (**2**), $[\mathrm{W_2Fe_6S_8(SR)_6(OMe)_3}]^{3-}$[17] (oxygen bridged, analogous to **2**), $[\mathrm{M_2Fe_7S_8(SR)_{12}}]^{3-,4-}$[13,18] (**3** and **4**); proposed octanuclear, $[\mathrm{Fe_4S_4(MoS_4)_4}]^{6-}$.[19] Those complexes with established structures[8,11-18] bear certain resemblances to the biological cluster based on conclusions from analysis of Mo EXAFS of native proteins and the FeMo cofactor,[2,3] which place as near neighbors to the Mo atom 3–4 S atoms at ~2.4 Å and 2–3 Fe atoms at ~2.7 Å. They contain one or more Fe···Mo interactions at 2.71–2.75 Å and two or more Mo–S bonds of 2.34–2.39 Å (2.25 Å in the binuclear species[8]). Although none of the synthetic clusters has a composition which corresponds to the 6–8 Fe/Mo atom ratio of the cofactor,[5,20] the resemblance of the Mo EXAFS of **1**–**3** to that of the enzyme is strongly suggestive of similar Mo coordination environments. In the course of developing the chemistry of $\mathrm{MoFe_3S_4}$ cluster complexes, we have previously reported the synthesis, detailed structures, and certain physical properties of **1** and **2**.[11,12] More recently, we have communicated similar information for the tri- and tetraanions **3** and **4** and their tungsten counterparts.[13,18] Here we describe the synthesis of the Mo and W clusters of types **3** and **4**, the W analogue of **1**, and a more complete set of spectroscopic and electrochemical properties of Mo and W clusters of types **1**–**4**.

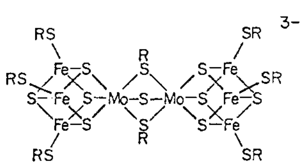

1

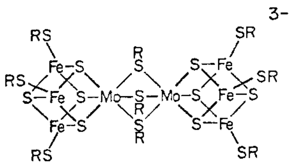

2

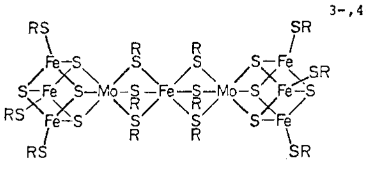

3 (3-), 4 (4-)

Experimental Section

Preparation of Compounds. Salts of $[\mathrm{Mo_2Fe_6S_9(SEt)_8}]^{3-}$ and $[\mathrm{Mo_2Fe_6S_8(SEt)_9}]^{3-}$ were prepared as previously described.[12] In the following preparations all steps were conducted under a pure dinitrogen atmosphere with degassed solvents. Percent yields are based on initial quantities of quaternary ammonium salts of $\mathrm{MS_4}^{2-}$ (M = Mo, W). The compounds were obtained from $\mathrm{(NH_4)_2MS_4}$ (M = Mo,[21] W[22]) by metathetical reactions with $\mathrm{R_4N^+}$ halide salts in acetonitrile ($\mathrm{Et_4N^+}$, $\mathrm{Et_3NCH_2Ph^+}$, n-$\mathrm{Bu_4N^+}$) or water ($\mathrm{Me_3NCH_2Ph^+}$). Description of a product as "pure" when it was not a part of an analytical sample means that its ^{1}H NMR spectrum contained no significant impurity resonances (see text).

$\mathrm{(Et_4N)_3[W_2Fe_6S_9(SEt)_8]}$. A slurry of 8.40 g (14.7 mmol) of $\mathrm{(Et_4N)_2WS_4}$ in 200 mL of methanol was added to the mixture formed by the addition of 132 mmol of sodium ethanethiolate (from 8.18 g of ethanethiol and 3.04 g of sodium) in 200 mL of methanol to a filtered solution of 7.20 g (44.4 mmol) of $\mathrm{FeCl_3}$ in 150 mL of methanol. After 12 h of stirring, volatile materials were removed in vacuo. The resultant black residue was extracted with 200 mL of acetonitrile, and the extract was filtered. The filtrate volume was reduced in vacuo to ca. 80 mL and was cooled to −20 °C for several hours. Black crystals were collected and recrystallized three times from minimum volumes of warm acetonitrile, affording 2.50 g (18%) of pure product as black crystals. Anal. Calcd for $\mathrm{C_{40}H_{100}Fe_6N_3S_{17}W_2}$: C, 25.68; H, 5.39; Fe, 17.91; N, 2.25; S, 29.13; W, 19.65. Found: C, 25.53; H, 5.28; Fe, 17.34; N, 2.30; S, 29.04; W, 19.71. Absorption spectrum (acetonitrile): $\lambda_{\max}$ 252 (sh) (ϵ_M 49 000), 389 (32 800) nm.

$\mathrm{(Me_3NCH_2Ph)_3[Mo_2Fe_7S_8(SEt)_{12}]}$. A solution of 13.7 g (221 mmol) of ethanethiol and 11.9 g (221 mmol) of sodium methoxide in 100 mL of methanol was added to a filtered solution of 10.4 g (64.4 mmol) of $\mathrm{FeCl_3}$ in 100 mL of methanol. To this mixture was added a slurry of 9.20 g (18.4 mmol) of $\mathrm{(Me_3NCH_2Ph)_2MoS_4}$ in 300 mL of methanol. The reaction system darkened to a brown color and microcrystalline material appeared within minutes. After overnight stirring the reaction product was collected by filtration. Washing with ethanol followed by drying in vacuo afforded 19.8 g of black solid. This material was extracted with ca. 700 mL of warm (50 °C) acetonitrile, and the extract was filtered. Reduction of the extract volume to 150 mL and cooling to −20 °C resulted in separation of 11.9 g (64%) of a black crystalline solid. One additional recrystallization from acetonitrile gave 8.94 g (48%) of pure product as black crystals. An analytical sample was recrystallized once more from acetonitrile. Anal. Calcd for $\mathrm{C_{54}H_{108}Fe_7Mo_2N_3S_{20}}$: C, 32.05; H, 5.38; Fe, 19.32; Mo, 9.48; N, 2.08; S, 31.69. Found: C, 31.95; H, 5.34; Fe, 19.41; Mo, 9.36; N, 2.10; S, 31.63. Absorption spectrum (acetonitrile): $\lambda_{\max}$ 281 (ϵ_M 77 000), 392 (58 900) nm.

$\mathrm{(Et_4N)_3[Mo_2Fe_7S_8(SEt)_{12}]}$. The procedure and molar ratios in the preceding preparation were utilized in the synthesis of this compound. The initial solid obtained from a reaction system based on 14.5 g (30 mmol) of $\mathrm{(Et_4N)_2MoS_4}$ and 750 mL of ethanol, after washing with ethanol and vacuum drying, was extracted with 300 mL of warm acetonitrile. The extract was filtered and its volume was reduced to ca. 100 mL. Addition of 150 mL of 1:1 (v/v) ether/THF and cooling to −20 °C caused separation of 23.1 g (78%) of pure product as black microcrystals. An analytical sample was recrystallized from the same solvent medium. Anal. Calcd for $\mathrm{C_{48}H_{120}Fe_7Mo_2N_3S_{20}}$: C, 29.34; H, 6.16; Fe, 19.91; Mo, 9.77; N, 2.14; S, 32.66. Found: C, 29.26; H, 6.13; Fe, 19.86; Mo, 9.56; N, 2.19; S, 32.47. Absorption spectrum (acetonitrile): $\lambda_{\max}$ 281 (ϵ_M 73 900), 394 (56 400) nm.

$\mathrm{(Me_3NCH_2Ph)_3[W_2Fe_7S_8(SEt)_{12}]}$. A slurry of 5.1 g (8.3 mmol) of $\mathrm{(Me_3NCH_2Ph)_3WS_4}$ in 100 mL of methanol was added to the mixture formed from the addition of 83 mmol of sodium ethanethiolate (from 5.2 g of ethanethiol and 1.9 g of sodium) in 200 mL of methanol to a filtered solution of 4.5 g (25 mmol) of $\mathrm{FeCl_3}$ in 200 mL of methanol. The reaction system was stirred for 20 h and cooled to −20 °C for 2 h. The black solid collected by filtration was extracted with successive portions of 200, 100, and 100 mL of acetonitrile. Reduction of the volume of the combined extracts in vacuo to ca. 80 mL afforded a black crystalline solid. Three recrystallizations of this material from acetonitrile gave 3.5 g (38%) of pure product as black crystals. Anal. Calcd for $\mathrm{C_{54}H_{108}Fe_7N_3S_{20}W_2}$: C, 29.49; H, 4.95; Fe, 17.77; N, 1.91; S, 29.16; W, 16.72. Found: C, 29.49; H, 4.49; Fe, 17.90; N, 2.09; S, 28.96; W, 16.94. Absorption spectrum (acetonitrile): $\lambda_{\max}$ 262 (ϵ_M 63 100), 390 (47 000) nm.

$\mathrm{(Et_4N)_3[W_2Fe_7S_8(SEt)_{12}]}$. This compound was prepared by using $\mathrm{(Et_4N)_2WS_4}$ in an ethanol reaction mixture. Otherwise the procedure and molar ratios were the same as in the preceding preparation. The pure product was obtained as black crystals in 35% yield after two recrystallizations from 1:1:2 (v/v/v) THF/ether/acetonitrile. Anal. Calcd for $\mathrm{C_{48}H_{120}Fe_7N_3S_{20}W_2}$: C, 26.95; H, 5.65; Fe, 18.27; N, 1.96; S, 29.98; W, 17.19. Found: C, 26.86, H, 5.49; Fe, 18.09; N, 2.07; S, 29.71; W, 17.38. Absorption spectrum (acetonitrile): $\lambda_{\max}$ 262 (ϵ_M 64 800), 389 (47 500) nm. An identical procedure with the exception of the use of $\mathrm{(Et_3NCH_2Ph)_2WS_4}$ yielded $\mathrm{(Et_3NCH_2Ph)_3[W_2Fe_7S_8(SEt)_{12}]}$ as a black crystalline product. This material was not analyzed but gave a ^{1}H NMR

---

[10] A Müller and S. Sarkar, *Angew. Chem., Int. Ed. Engl.*, **16**, 705 (1977).

[11] T. E. Wolff, J. M. Berg, C. Warrick, K. O. Hodgson, R. H. Holm, and R. B. Frankel, *J. Am. Chem. Soc.*, **100**, 4630 (1978).

[12] T. E. Wolff, J. M. Berg, K. O. Hodgson, R. B. Frankel, and R. H. Holm, *J. Am. Chem. Soc.*, **101**, 4140 (1979).

[13] T. E. Wolff, J. M. Berg, P. P. Power, K. O. Hodgson, R. H. Holm, and R. B. Frankel, *J. Am. Chem. Soc.*, **101**, 5454 (1979).

[14] G. Christou, C. D. Garner, F. E. Mabbs, and T. J. King, *J. Chem. Soc., Chem. Commun.*, 740 (1978).

[15] G. Christou, C. D. Garner, F. E. Mabbs, and M. G. B. Drew, *J. Chem. Soc., Chem. Commun.*, 91 (1979).

[16] (a) S. R. Acott, G. Christou, C. D. Garner, T. J. King, F. E. Mabbs, and R. M. Miller, *Inorg. Chim. Acta*, **35**, L337 (1979); (b) G. Christou, C. D. Garner, R. M. Miller, and T. J. King, *J. Inorg. Biochem.*, **11**, 349 (1979).

[17] G. Christou, C. D. Garner, T. J. King, C. E. Johnson, and J. D. Rush, *J. Chem. Soc., Chem. Commun.*, 503 (1979).

[18] T. E. Wolff, J. M. Berg, P. P. Power, K. O. Hodgson, and R. H. Holm, *Inorg. Chem.*, **19**, 430 (1980).

[19] H. C. Silvis, R. H. Tiecklemann, and B. A. Averill, *Inorg. Chim. Acta*, **36**, L423 (1979).

[20] V. K. Shah and W. J. Brill, *Proc. Natl. Acad. Sci. U.S.A.*, **74**, 3249 (1977); B. K. Burgess, D. B. Jacobs, and E. I. Stiefel, *Biochim. Biophys. Acta*, in press.

[21] G. Krüss, *Justus Liebigs Ann. Chem.*, **225**, 6 (1884).

[22] E. Corleis, *Justus Liebigs Ann. Chem.*, **232**, 244 (1886).

spectrum containing the same anion resonances as the preceding two compounds.

$(n\text{-Bu}_4N)_4[Mo_2Fe_7S_8(SCH_2Ph)_{12}]$. A solution of 8.5 g (12 mmol) of $(n\text{-Bu}_4N)_2MoS_4$ in 200 mL of ethanol was added to the mixture formed by the addition of 150 mmol of sodium benzylthiolate (from 18.6 g of benzylthiol and 3.5 g of sodium) in 150 mL of ethanol to a filtered solution of 6.8 g (42 mmol) of $FeCl_3$ in 150 mL of ethanol. After 6 h of stirring, the reaction mixture consisted of a pale red solution and ca. 20 g of a greenish solid, which was collected by filtration. Examination by ^1H NMR of an acetonitrile extract of this material revealed that the main soluble species was the desired product but was contaminated with $[Fe_4S_4(SCH_2Ph)_4]^{2-}$ and $[Mo_2Fe_7S_8(SCH_2Ph)_{12}]^{3-}$. Stirring the green solid overnight with 50 mL of a HMPA solution containing 1.5 mmol of sodium acenaphthalenide caused reduction of both species and removal of $[Fe_4S_4(SCH_2Ph)_4]^{3-}$ by preferential solubility. After the slurry was filtered the collected solid was washed with ethanol and dried in vacuo. Extraction of the solid with 200 mL of warm acetonitrile followed by filtration and cooling of the filtrate to −20 °C caused separation of 4.9 g of a black crystalline solid, which was collected by filtration. Recrystallization of this material from 140 mL of warm acetonitrile gave 3.7 g (19%) of the pure product as black crystals. Anal. Calcd for $C_{148}H_{228}Fe_7Mo_2N_4S_{20}$: C, 54.07; H, 6.99; Fe, 11.89; Mo, 5.84; N, 1.70; S, 19.51. Found: C, 54.46; H, 6.19; Fe, 11.92; Mo, 5.75; N, 1.78; S, 19.58. Absorption spectrum (acetonitrile): λ_{max} 288 (sh) (ϵ_M 90 900), 395 (50 600) nm.

$(n\text{-Bu}_4N)_4[W_2Fe_7S_8(SCH_2Ph)_{12}]$. A solution of 4.01 g (7.25 mmol) of $(n\text{-Bu}_4N)_2WS_4$ in 150 mL of methanol was added to the mixture formed by the addition of 70 mmol of sodium benzylthiolate (from 8.68 g of benzylthiol and 1.61 g of sodium) in 150 mL of methanol to a filtered solution of 3.41 g (21 mmol) of $FeCl_3$ in 150 mL of methanol. The reaction mixture was stirred for 4.5–5 h, maintained at −20 °C for 1 h, and filtered to yield a dark blue-green solid and a pale red-brown filtrate. The solid was extracted with successive portions of 100, 100, and 150 mL of acetonitrile. The filtered, intense green-brown extracts were combined. Reduction of the extract volume in vacuo to ca. 100 mL followed by cooling at −20 °C overnight afforded 5.1 g (41%) of the black crystalline product. The product was purified by two further recrystallizations from acetonitrile and was obtained as black crystals. Anal. Calcd for $C_{148}H_{228}Fe_7N_4S_{20}W_2$: C, 51.32; H, 6.63; Fe, 11.29; N, 1.61; S, 18.52; W, 10.62. Found: C, 51.20; H, 6.56; Fe, 11.11; N, 1.77; S, 18.31; W, 10.88. Absorption spectrum (acetonitrile): λ_{max} 257 (sh) (ϵ_M 97 000), 384 (44 200) nm.

$(Et_4N)_4[W_2Fe_7S_8(SEt)_{12}]$. A suspension of 4.15 g (7.25 mmol) of $(Et_4N)_2WS_4$ in 100 mL of ethanol was added to a slurry prepared by the addition of 72.5 mmol of sodium ethanethiolate (from 4.50 g of ethanethiol and 1.73 g of sodium) to a filtered solution of 3.53 g (21.8 mmol) of $FeCl_3$ in 100 mL of ethanol. The reaction mixture was stirred for 18 h and allowed to stand at −20 °C for 2 h, and the black crystalline product was collected by filtration. This material was purified by two recrystallizations from acetonitrile/THF/ether. Contamination with the oxidation product $(Et_4N)_3[W_2Fe_7S_8(SEt)_{12}]$, which is difficult to separate from the desired compound by crystallization, can be avoided by adhering to the specified quantities of solvents and reactants and by rigorously excluding dioxygen. Small amounts of oxidation product, detectable by ^1H NMR (see text), can be reduced by washing the recrystallized product with small portions (e.g., 2 × 20 mL) of a 1 mM solution of sodium acenaphthalenide in HMPA, followed by washing with ethanol and removal of any residual solvent in vacuo. These procedures typically afforded 2.4 g (30%) of pure product as black crystals. Anal. Calcd for $C_{56}H_{140}Fe_7N_4S_{20}W_2$: C, 29.64; H, 6.22; Fe, 17.22; N, 2.47; S, 28.25; W, 16.20. Found: C, 29.63; H, 6.16; Fe, 17.44; N, 2.60; S, 28.07; W, 16.11. Absorption spectrum (acetonitrile): λ_{max} 257 (ϵ_M 76 500), 380 (49 200) nm. The pure $n\text{-Pr}_4N^+$ salt was obtained in a similar manner except that methanol was employed as the reaction solvent.

Physical Measurements. Owing to the oxygen sensitivity of the compounds, all measurements were performed under an inert atmosphere; solvents were dried and thoroughly degassed. Electronic absorption spectra were recorded on a Cary Model 219 spectrophotometer. ^1H NMR spectra were recorded in the Fourier transform mode on a Varian XL-100-15 or a modified Bruker HXS-360 spectrometer equipped with the temperature control and data acquisition and processing systems described previously.[23] Acetonitrile-d_3 (99%) was distilled from calcium hydride. Isotropic shifts were calculated from the relationship $(\Delta H/H_0)_{iso} = (\Delta H/H_0)_{obsd} - (\Delta H/H_0)_{dia}$, in which the diamagnetic reference shifts are those of the appropriate thiols in CD_3CN[24] and the observed shifts were measured relative to Me_4Si. Following the usual convention for paramagnetic molecules, observed and reference shifts are taken as negative when occurring downfield from Me_4Si. Cyclic voltammetry was performed with solutions containing 0.05 M $(n\text{-Bu}_4N)(BF_4)$ supporting electrolyte, a glassy carbon working electrode, a platinum wire auxiliary electrode, and instrumentation already described.[25] Potentials were measured at ambient temperature vs. a saturated calomel electrode (SCE). Mössbauer spectra (^{57}Fe) in zero and applied magnetic fields were obtained with a constant-acceleration spectrometer with the source (^{57}Co in Rh) maintained at the same temperature as the absorber. Samples were examined as crystalline absorbers dispersed in boron nitride powder. Isomer shifts are relative to iron metal at the same temperature (to refer to iron metal at room temperature 0.12 mm/s should be added to the quoted shifts). Magnetic susceptibility determinations of crystalline solids were carried out with a SQUID-type susceptometer previously described.[26]

Results and Discussion

The anaerobic reaction system (1) (M = Mo, W; R = Et, CH$_2$Ph) as conducted in this laboratory affords four principal types[27] of "double-cubane" cluster anions, which are isolable as quaternary ammonium salts and possess the indicated structures.[11-13,18] Relative yields of specific types have been increased by empirical variation of R substituent, cation, solvent, and reaction time; desired products are purified by fractional recrystallization. The synthetic procedures given here and elsewhere[12] reflect variation of these reaction parameters and represent our best current attempts to optimize yields. Analogous Mo and W complexes of each of the four types of cluster anions **1**–**4** have been obtained except for type **2**, where only $[Mo_2Fe_6S_8(SEt)_9]^{3-}$ has been isolated. Using a similar reaction system, Christou, Garner, and co-workers have isolated and structurally characterized a series of $[Mo_2Fe_6S_8(SR)_9]^{3-}$ species (R = Ph,[14] CH$_2$CH$_2$OH,[15] Et[16a]) as well as $[W_2Fe_6S_8(SEt)_9]^{3-}$ [16b] and $[W_2Fe_6S_8(SPh)_6(OMe)_3]^{3-}$.[17]

$$MS_4^{2-} + 3\text{–}3.5FeCl_3 + 9\text{–}12NaSR \xrightarrow[\sim 25\ ^\circ C]{MeOH,EtOH} \qquad (1)$$

$$\underset{\mathbf{1}}{[M_2Fe_6S_9(SEt)_8]^{3-}}$$

$$\underset{\mathbf{2}}{[Mo_2Fe_6S_8(SEt)_9]^{3-}}$$

$$\underset{\mathbf{3}}{[M_2Fe_7S_8(SEt)_{12}]^{3-}}$$

$$\underset{\mathbf{4}}{[W_2Fe_7S_8(SEt)_{12}]^{4-}},\ \underset{\mathbf{4}}{[M_2Fe_7S_8(SCH_2Ph)_{12}]^{4-}}$$

The structures of $[Mo_2Fe_6S_9(SEt)_8]^{3-}$ [11,12] (**1**), $[Mo_2Fe_6S_8(SEt)_9]^{3-}$ [12] (**2**), $[Mo_2Fe_7S_8(SEt)_{12}]^{3-}$ [13,18] (**3**), and $[M_2Fe_7S_8(SCH_2Ph)_{12}]^{4-}$ [13,18] (**4**), together with the zero-field Mössbauer properties of the first two species,[12] have been described in detail earlier. Significant structural features include the presence of essentially isodimensional MFe_3S_4 cores in *all* species and the presence of bridging Fe^{III} and Fe^{II} in **3** and **4**, respectively. Here we examine absorption, ^{57}Fe Mössbauer, and ^1H NMR spectra and voltammetric behavior in an initial attempt to probe the electronic and redox properties of cluster anions **1**–**4**.

UV–Visible Spectra. A feature apparently characteristic of the $MFe_3S_4(SR)_3$ clusters possessing the oxidation levels in **1**–**4** (vide infra) is the appearance of well-resolved bands at 391–396 (M = Mo) and 384–390 (M = W) nm in acetonitrile solution. In addition, a second feature is found at 266–288 and 252–262 nm in the Mo and W spectra, respectively. Spectra of Mo and W complexes of types **3** and **4** are shown in Figure 1; those of Mo

---

[23] J. G. Reynolds, E. J. Laskowski, and R. H. Holm, *J. Am. Chem. Soc.*, **100**, 5315 (1978).

[24] R. H. Holm, W. D. Phillips, B. A. Averill, J. J. Mayerle, and T. Herskovitz, *J. Am. Chem. Soc.*, **96**, 2109 (1974).

[25] J. Cambray, R. W. Lane, A. G. Wedd, R. W. Johnson, and R. H. Holm, *Inorg. Chem.*, **16**, 2565 (1977).

[26] E. J. Laskowski, R. B. Frankel, W. O. Gillum, G. C. Papaefthymiou, J. Renaud, J. A. Ibers, and R. H. Holm, *J. Am. Chem. Soc.*, **100**, 5322 (1978).

[27] Minority species, exhibiting paramagnetically shifted ^1H NMR signals, have been observed in several reaction systems but have not been isolated or identified.

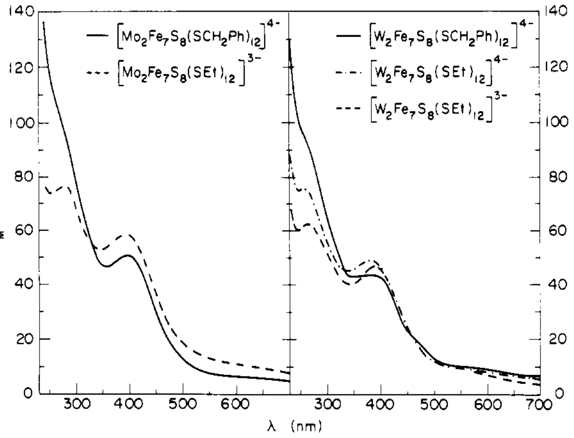

Figure 1. Electronic absorption spectra of $[\mathrm{M_2Fe_7S_8(SEt)_{12}}]^{3-}$, $[\mathrm{M_2Fe_7S_8(SCH_2Ph)_{12}}]^{4-}$, and $[\mathrm{W_2Fe_7S_8(SEt)_{12}}]^{4-}$ in acetonitrile solutions at ambient temperature (M = Mo, W).

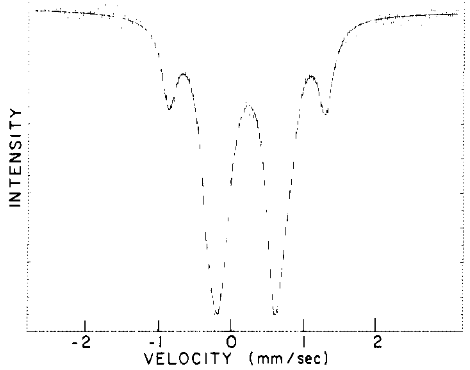

Figure 2. ^{57}Fe Mössbauer spectrum of $(\mathrm{Et_4N})_3[\mathrm{Mo_2Fe_7S_8(SEt)_{12}}]$ at 77 K.

complexes **1** and **2** have been given elsewhere.[12] The spectra are similar in appearance to those of $[\mathrm{Fe_4S_4(SR)_4}]^{2-}$ clusters with the same R substituent[28] and, as in those cases, presumably arise from RS → core charge-transfer excitations. Apart from the greater intensities of the bands in type **3** and **4** clusters the spectra are of marginal utility in identification of purity assay of **1–4**, which is best accomplished by ^{1}H NMR spectroscopy (vide infra).

Mössbauer Spectra. Spectral parameters at 77 K for the W cluster **1** and the Mo and W clusters **3** and **4**, obtained by computer fitting of the experimental spectra with Lorentzian line shapes, are collected in Table I. Spectra of the type **3** complexes, exemplified by that of $(\mathrm{Et_4N})_3[\mathrm{Mo_2Fe_7S_8(SEt)_{12}}]$ in Figure 2, consist of two resolved quadrupole doublets while those of type **4** complexes, represented by that of $(n\text{-}\mathrm{Bu_4N})_4[\mathrm{Mo_2Fe_7S_8(SCH_2Ph)_{12}}]$ in Figure 3, are similar but one component of the less intense doublet is not resolved. The latter features are assigned to the Fe atoms in the $\mathrm{Fe(SR)_6}$ bridge units of types **3** and **4**. Assuming equivalent recoilless fractions, the bridge to core Fe intensity ratio should be 1:6, close to the majority of observed values. Moreover, the less intense doublet is absent in the spectra of type **1** and **2** clusters. Isomer shifts suffice to identify the oxidation states of the bridging Fe atoms. The values for type **3** clusters (0.31 mm/s) are consistent with the range 0.29–0.39 mm/s found for mainly low-spin $\mathrm{Fe^{III}S_6}$ species.[29–31] In particular, the isomer shift of low-spin $\mathrm{Fe^{III}}$ [32] in $\{[\mathrm{Co(H_2NCH_2CH_2S)_3}]_2\mathrm{Fe}\}^{3+}$,[30] which presumably provides a bridging environment quite similar to that in type **3** clusters, is ~0.29 mm/s at 104 K. Shifts of type **4** clusters (0.81, 0.85 mm/s) are larger and lie on the low end of the 0.86–0.93 mm/s range[31] found for tris(xanthato) and -(dithiocarbamato) complexes containing high-spin $\mathrm{Fe^{II}S_6}$ units.[33] These oxidation state assignments accord with those deduced from $\mathrm{Fe(SR)_6}$ bridge structural features in $[\mathrm{Mo_2Fe_7S_8(SEt)_{12}}]^{3-}$ and $[\mathrm{M_2Fe_7S_8(SCH_2Ph)_{12}}]^{4-}$.[18]

Table I. Mössbauer Spectral Parameters at 77 K

compd	δ,[a] mm/s	ΔE_Q,[b] mm/s	rel intens
$(\mathrm{Et_4N})_3[\mathrm{W_2Fe_6S_9(SEt)_8}]$	0.32	1.05	
$(\mathrm{Et_4N})_3[\mathrm{Mo_2Fe_7S_8(SEt)_{12}}]$	0.29 0.32	0.78 1.17	5.8
	0.31	2.18	1.0
$(\mathrm{Me_3NCH_2Ph})_3[\mathrm{Mo_2Fe_7S_8(SEt)_{12}}]$	0.29 0.32	0.74 1.10	6.0
	0.31	2.13	1.0
$(\mathrm{Et_4N})_3[\mathrm{W_2Fe_7S_8(SEt)_{12}}]$	0.31 0.31	0.88 1.19	6.8
	0.31	2.16	1.0
$(n\text{-}\mathrm{Bu_4N})_4[\mathrm{Mo_2Fe_7S_8(SCH_2Ph)_{12}}]$	0.30	0.96	5.8
	0.85[c]	1.90[c]	1.0
$(n\text{-}\mathrm{Bu_4N})_4[\mathrm{W_2Fe_7S_8(SCH_2Ph)_{12}}]$	0.33	1.08	~8.0
	0.81[c]	2.02[c]	1.0

[a] Relative to Fe metal at 77 K; ±0.02 mm/s unless noted otherwise. [b] ±0.03 mm/s unless noted otherwise. [c] ±0.06 mm/s; these larger uncertainties arise from partial overlap of spectral features.

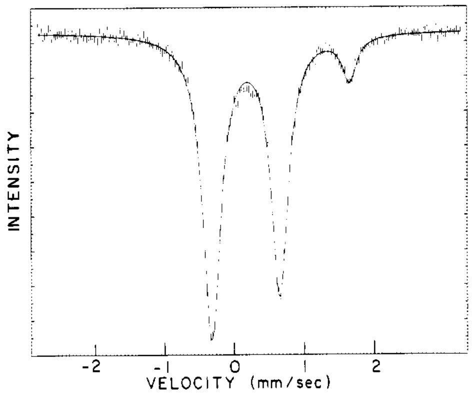

Figure 3. ^{57}Fe Mössbauer spectrum of $(n\text{-}\mathrm{Bu_4N})_4[\mathrm{Mo_2Fe_7S_8(SCH_2Ph)_{12}}]$ at 77 K.

The more intense doublet in the spectrum of each cluster arises from the Fe atoms of the $\mathrm{MFe_3S_4}$ core. Parameters of this spectral feature are quite similar to those found for $[\mathrm{Mo_2Fe_6S_9(SEt)_8}]^{3-}$ and $[\mathrm{Mo_2Fe_6S_8(SEt)_9}]^{3-}$ [12] and exhibit no significant dependence on the identity of the M atom or the nature of the bridging structure. Isomer shifts at 77 K of all cluster types **1–4** thus far examined occur in the narrow interval 0.27–0.33 mm/s, a result strongly suggestive of the same average oxidation state of Fe atoms in each cluster. On the basis of trends in isomer shifts of complexes containing tetrahedral $\mathrm{FeS_4}$ units[12] (ranging from $\mathrm{Fe^{II}}$ to $\mathrm{Fe^{III}}$) and in terminal and bridging Fe–S distances in clusters,[12,18] we conclude that the Fe atoms in **1–4** are certainly more oxidized than in $[\mathrm{Fe_4S_4(SR)_4}]^{3-}$ ($\mathrm{Fe^{III}} + 3\mathrm{Fe^{II}}$) and probably more oxidized than in $[\mathrm{Fe_4S_4(SR)_4}]^{2-}$ ($2\mathrm{Fe^{III}} + 2\mathrm{Fe^{II}}$). Consequently, we favor the mean oxidation state description $\mathrm{Fe^{2.67+}}$ ($2\mathrm{Fe^{III}} + \mathrm{Fe^{II}}$) in cluster types **1–4**.

Spectral fitting results for several $[\mathrm{M_2Fe_7S_8(SEt)_{12}}]^{3-}$ salts indicate that core Fe atoms are nearly but not exactly electronically equivalent at 77 K (Table I), a situation not inconsistent with the

---

(28) B. V. DePamphilis, B. A. Averill, T. Herskovitz, L. Que, Jr., and R. H. Holm, *J. Am. Chem. Soc.*, **96**, 4159 (1974).

(29) L. M. Epstein and D. K. Straub, *Inorg. Chem.*, **8**, 784 (1969); P. B. Merrithew and P. G. Rasmussen, *ibid.*, **11**, 325 (1972); R. Richards, C. E. Johnson, and H. A. O. Hill, *J. Chem. Soc. A*, 797 (1971).

(30) G. Freeh, K. Chapman, and E. Blinn, *Inorg. Nucl. Chem. Lett.*, **9**, 91 (1973).

(31) Where appropriate literature δ values have been corrected to Fe metal reference at 77–100 K for comparison with the data in Table I.

(32) R. E. DeSimone, T. Ontko, L. Wardman, and E. L. Blinn, *Inorg. Chem.*, **14**, 1313 (1975).

(33) J. L. K. F. de Vries, J. M. Trooster, and E. de Boer, *Inorg. Chem.*, **12**, 2730 (1973); C. A. Yong, B. W. Fitzsimmons, L. F. Larkworthy, and S. E. Al-Muktar, *Inorg. Chim. Acta*, **33**, 249 (1979).

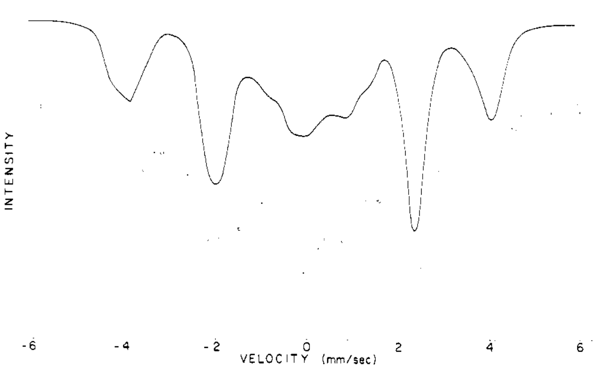

Figure 4. ^{57}Fe Mössbauer spectrum of $(Et_4N)_3[Mo_2Fe_7S_8(SEt)_{12}]$ at 4.2 K and H_0 = 80 kOe. The solid line is a theoretical simulation of the experimental spectrum (O) assuming in each $MoFe_3S_4$ core Fe subsites with 2:1 relative intensity and parameters given in the text. The spectrum of the bridge Fe atom is obscured by that of the core Fe atoms.

crystallographic imposition of only centrosymmetry on the anion in $(Me_3NCH_2Ph)_3[Mo_2Fe_7S_8(SEt)_{12}]$.[18] When examined in applied longitudinal magnetic fields, the spectra of $(Et_4N)_3[Mo_2Fe_7S_8(SEt)_{12}]$ at $H_0 < 40$ kOe exhibit broad, poorly resolved lines. At high fields ($40 \leq H_0 \leq 80$ kOe) the spectra are resolved into two subspectra with relative integrated intensities of ca. 2:1. The 80-kOe spectrum is shown in Figure 4 with a computer simulation assuming a field gradient of 1.2 mm/s, an asymmetry parameter $\eta = 0.5$, and the sign of the principal component of the **efg** tensor negative at both sites. Magnetic fields at the nuclei are $|H_n|$ = 114 and 230 kOe for the more intense and less intense subsites, respectively. From variation in line splittings with applied H_0 it is inferred that the hyperfine magnetic fields at 80 kOe are −194 kOe for the more intense and +154 kOe for the less intense subsites.[34] Similar magnetic field spectra have been observed for $(Et_4N)_3[Mo_2Fe_6S_9(SEt)_8]$, $(Et_3NCH_2Ph)_3[Mo_2Fe_6S_8(SEt)_9]$, $(Me_3NCH_2Ph)_3[Mo_2Fe_7S_8(SEt)_{12}]$, and $(n\text{-}Bu_4N)_4[Mo_2Fe_7S_8(SCH_2Ph)_{12}]$, except for slightly different hyperfine interactions and line widths. In the first of these compounds, for example, subsite intensities are ca. 2:1, with hyperfine magnetic fields at 80 kOe being −210 and +150 kOe for the more intense and less intense subsites, respectively. It is likely that core Fe inequivalence is an intrinsic electronic property of all clusters **1–4**, at least at $T \leq 77$ K, for it has been observed in all magnetically perturbed spectra examined thus far. Crystallographic structural equivalence of Fe atoms (at ambient temperature), as in $(Et_3NCH_2Ph)_3[Mo_2Fe_6S_8(SEt)_9]$,[12] does not necessarily imply strict electronic equivalence, inasmuch as more than one subsite is observable even in the zero-field spectrum of this compound. Subsites have also been reported in $(Et_4N)_3[W_2Fe_6S_8(SPh)_6(OMe)_3]$ from its Mössbauer spectrum at 77 K.[17]

The observation of magnetic hyperfine structure induced by external fields means that the electronic ground states of the clusters are paramagnetic and there is unpaired spin at all core Fe atoms. Moreover, the two magnetic subsites with different hyperfine interactions of opposite sign and ca. 2:1 relative intensities imply antiparallel spin coupling within each cluster, with the more intense subsite corresponding to the majority spin direction. This latter observation is consistent with the spin structures of $[Fe_4S_4(SR)_4]^{3-}$ clusters,[26,35] where antiparallel spin configurations are also observed. By analogy with those clusters, we would expect the Mo spin to be coupled to the minority iron spin in each cluster. At high fields, the moments of the two clusters in each anion are oriented parallel to each other. Paramagnetic ground states and negative temperature coefficients of magnetic susceptibility have been confirmed by magnetic measurements at 4.2–337 K.[36]

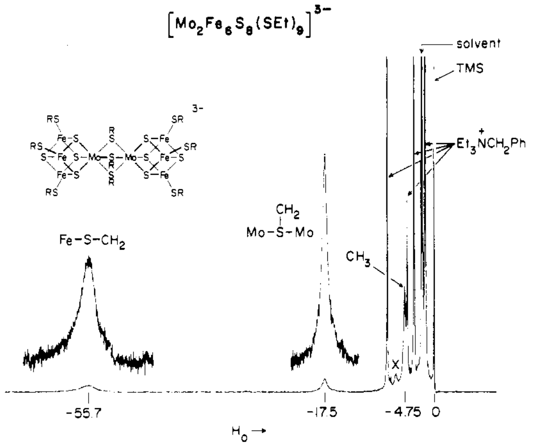

Figure 5. ^{1}H FT NMR spectrum (360 MHz) of $(Et_3NCH_2Ph)_3[Mo_2Fe_6S_8(SEt)_9]$ in CD_3CN at ~22 °C. Signal assignments are indicated (X = impurity).

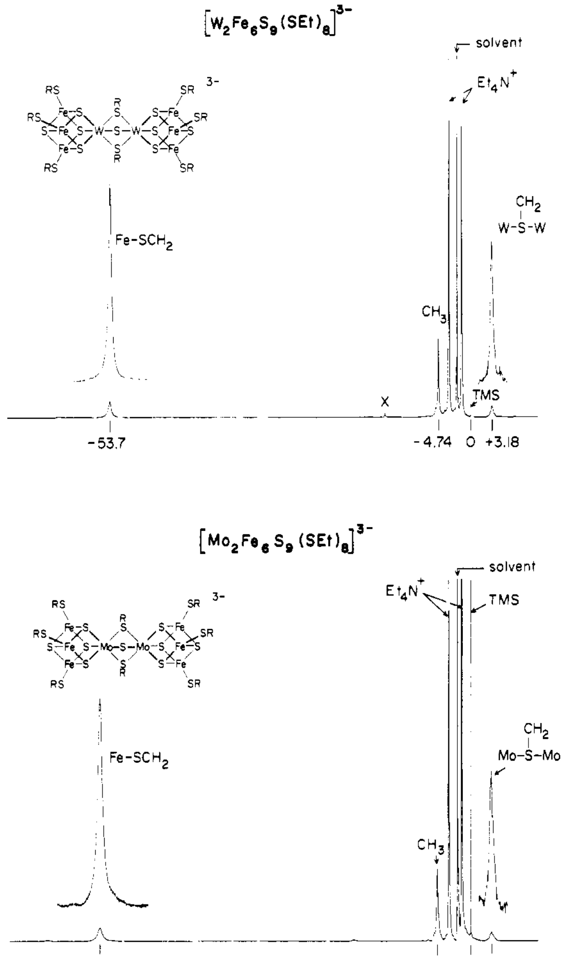

Figure 6. ^{1}H FT NMR spectra (360 MHz) of $(Et_4N)_3[M_2Fe_6S_9(SEt)_8]$ (M = Mo, W) in CD_3CN at ~22 °C. Signal assignments are indicated.

^{1}H NMR Spectra. These spectra provide several types of important information, among which is compound identification and assessment of purity. Inasmuch as the reaction systems tend to afford more than one cluster species and the only satisfactory

---

[34] Magnetization measurements at 4.2 K show that the magnetic moment is still increasing at 54 kOe (M/μ_B = 4.22), indicating that the hyperfine interactions may be expected to be field-dependent at even higher fields.

[35] E. J. Laskowski, J. G. Reynolds, R. B. Frankel, S. Foner, G. C. Papaefthymiou, and R. H. Holm, *J. Am. Chem. Soc.*, **101**, 6562 (1979).

[36] The following data ($10^3\chi_M$, μ (μ_B)) at 4.3, 100, and 299 K illustrate magnetic behavior. $(Et_4N)_3[Mo_2Fe_6S_9(SEt)_8]$: 706, 4.87; 40.1, 5.67; 14.2, 5.83. $(Et_3NCH_2Ph)_3[Mo_2Fe_6S_8(SEt)_9]$: 910, 5.62; 38.3, 5.54; 13.7, 5.73. $(Me_3NCH_2Ph)_3[Mo_2Fe_7S_8(SEt)_{12}]$: 764, 5.15; 39.8, 5.65; 14.1, 5.80. Because of the complexity of these spin-coupled systems we cannot provide a satisfactory interpretation of $\chi_M(T)$ behavior of clusters **1–4** and thus defer reporting the full body of magnetic data.

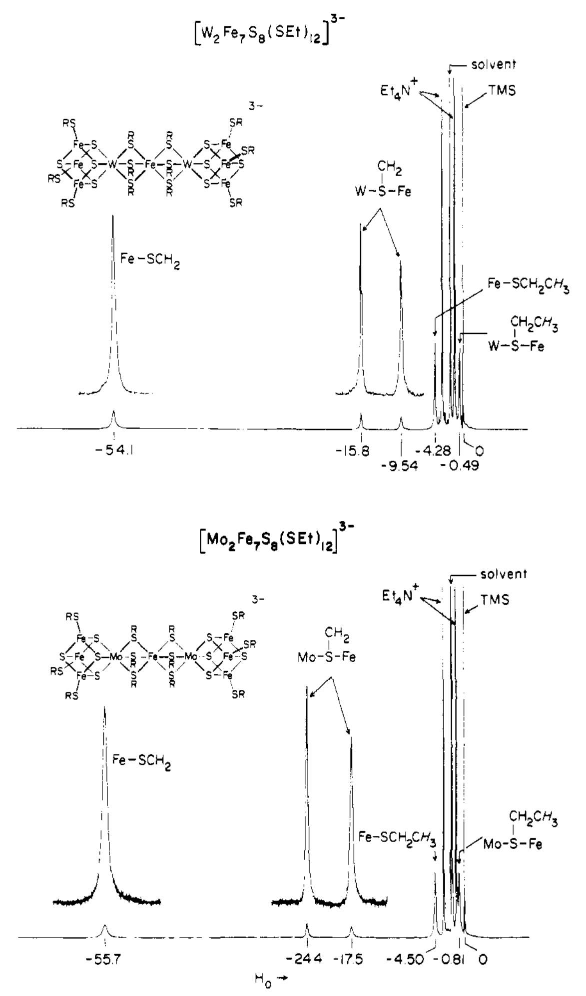

Figure 7. ^{1}H FT NMR spectra (360 MHz) of $(Et_4N)_3[M_2Fe_7S_8(SEt)_{12}]$ (M = Mo, W) in CD_3CN at ~22 °C. Signal assignments are indicated.

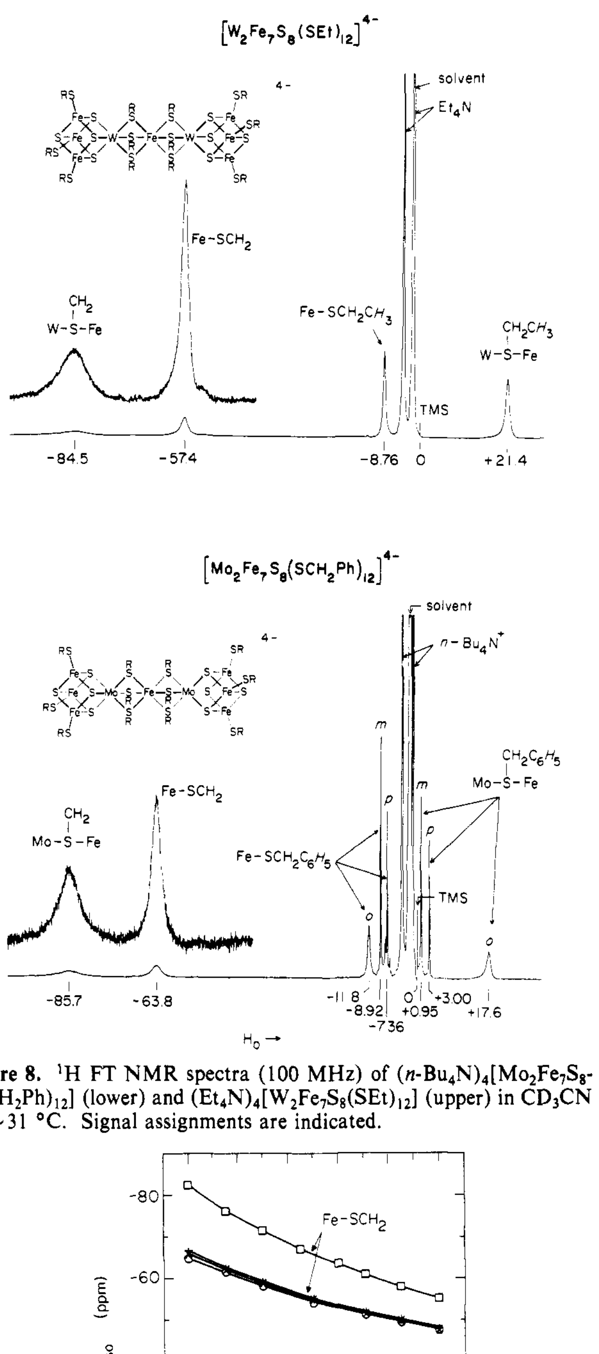

Figure 8. ^{1}H FT NMR spectra (100 MHz) of $(n\text{-}Bu_4N)_4[Mo_2Fe_7S_8(SCH_2Ph)_{12}]$ (lower) and $(Et_4N)_4[W_2Fe_7S_8(SEt)_{12}]$ (upper) in CD_3CN at ~31 °C. Signal assignments are indicated.

method for purification thus far devised is fractional crystallization, ^{1}H NMR spectroscopy has proven indispensable in identifying mixtures and (together with analytical data) affording criteria for satisfactory purity. Absorption and Mössbauer spectroscopy and electrochemistry (vide infra) are not adequate in this respect. For this reason spectra of satisfactorily pure compounds containing examples of cluster types **1**–**4** are presented in Figures 5–8.

A. Assignments. Because clusters **1**–**4** are paramagnetic, resonances are isotropically shifted. Most assignments given in the figures are straightforward and follow from relative signal intensities and chemical results. Reactions of the clusters with 6 equiv of acetyl chloride, a reagent previously demonstrated to replace terminal thiolate groups with chloride in $[Fe_4S_4(SR)_4]^{2-}$,[37] abolish all signals assigned to $Fe-SCH_2CH_3$ groups. The remaining signals, which therefore arise from bridging thiolate groups, are unaffected in relative intensities and experience changes in chemical shift.[38] Thus as a consequence of reaction 2 signals

$$\underset{\mathbf{(2)}}{[Mo_2Fe_6S_8(SEt)_9]^{3-}} + 6CH_3COCl \rightarrow [Mo_2Fe_6S_8Cl_6(SEt)_3]^{3-} + 6CH_3COSEt \quad (2)$$

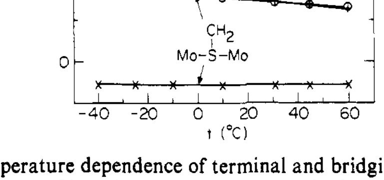

Figure 9. Temperature dependence of terminal and bridging SCH_2 isotropic shifts in CD_3CN solution: (□) $[Mo_2Fe_7S_8(SCH_2Ph)_4]^{4-}$; (+) $[Mo_2Fe_7S_8(SEt)_{12}]^{3-}$; (×) $[Mo_2Fe_6S_9(SEt)_8]^{3-}$; (○) $[Mo_2Fe_6S_8(SEt)_9]^{3-}$.

at −55.7 and −4.75 ppm are eliminated and that at −17.5 ppm (Figure 5) is shifted to −18.4 ppm. The spectra in Figure 6 are similarly affected, with the bridging methylene resonances displaced several ppm upfield as a result of chloride substitution. However, in 100- and 360-MHz spectra of $[M_2Fe_6S_9(SEt)_8]^{3-}$ the methyl resonance of the bridging ethanethiolate groups could not be located and apparently is obscured by solvent or cation signals. In reaction 3 signals at −55.7 and −4.50 ppm (M = Mo) and at

$$\underset{\mathbf{(3)}}{[M_2Fe_7S_8(SEt)_{12}]^{3-}} + 6CH_3COCl \rightarrow [M_2Fe_7S_8Cl_6(SEt)_6]^{3-} + 6CH_3COSEt \quad (3)$$

−54.1 and −4.28 ppm (M = W, Figure 7) are removed and the

---

[37] G. B. Wong, M. A. Bobrik, and R. H. Holm, *Inorg. Chem.*, **17**, 578 (1978); R. W. Johnson and R. H. Holm, *J. Am. Chem. Soc.*, **100**, 5338 (1978).

[38] R. E. Palermo, C. L. Coyle, P. P. Power, and R. H. Holm, research in progress.

Table II. ^1H Isotropic Shifts in CD_3CN Solution at Ambient Temperature

complex	position	$(\Delta H/H_0)_{iso}$,[a] ppm terminal	$(\Delta H/H_0)_{iso}$,[a] ppm bridge
$[Mo_2Fe_6S_9(SEt)_8]^{3-}$	CH_2	−52.8	+5.64
	CH_3	−3.69	*c*
$[W_2Fe_6S_9(SEt)_8]^{3-}$	CH_2	−51.2	+5.69
	CH_3	−3.47	*c*
$[Mo_2Fe_6S_8(SEt)_9]^{3-}$	CH_2	−53.2	−15.0
	CH_3	−3.48	*c*
$[Mo_2Fe_6S_8(SPh)_9]^{3-}$	*o*-H	+10.3	−1.42
	m-H	−6.61	+1.33
	p-H	+10.9	+1.90
$[Mo_2Fe_7S_8(SEt)_{12}]^{3-}$	CH_2	−53.2	−21.9, −15.0
	CH_3	−3.23	+0.46
$[W_2Fe_7S_8(SEt)_{12}]^{3-}$	CH_2	−51.6	−13.3, −7.03
	CH_3	−3.01	+0.78
$[W_2Fe_7S_8(SEt)_{12}]^{4-}$	CH_2	−54.9	−82.0[d]
	CH_3	−7.49	+22.7
$[Mo_2Fe_7S_8(SCH_2Ph)_{12}]^{4-}$ [b]	CH_2	−60.2	−82.1[d]
	o-H, *m*-H	−4.65, −1.77	+24.8, +8.10
	p-H	−0.21	+10.2
$[W_2Fe_7S_8(SCH_2Ph)_{12}]^{4-}$ [b]	CH_2	−56.3	−79.3[d]
	o-H, *m*-H	−4.18, −1.54	+23.1, +7.74
	p-H	−0.09	+9.23

[a] Determined at 22 °C unless otherwise noted. [b] 31 °C. [c] Not located. [d] Exchange-averaged signal.

downfield pairs of signals which remain are shifted to −26.3, −38.4 ppm (M = Mo) and −17.8, −26.3 ppm (M = W). These results demonstrate that $[Mo_2Fe_7S_8(SEt)_{12}]^{3-}$ possesses two bridge methylene signals, one of which is accidentally degenerate in chemical shift at 22 °C with the bridge methylene resonance of $[Mo_2Fe_6S_8(SEt)_9]^{3-}$. The temperature dependencies of these signals, shown in Figure 9, are different at lower temperatures. Spectra of the $[M_2Fe_7S_8(SR)_{12}]^{4-}$ clusters (Figure 8) could be completely assigned on the basis of relative intensities. Full details of the reactions of the clusters with acetyl chloride and other electrophiles, including demonstration that the hexachloride species can be reversibly reconstituted to precursors or substituted to form different thiolate complexes with retention of core + bridge structures, will be reported subsequently.[38]

B. Isotropic Interactions. The dominant magnetic interactions affording the isotropically shifted spectra of cluster types **1**–**4** can be recognized from the collection of isotropic shifts $[(\Delta H/H_0)_{iso} = (\Delta H/H_0)_{con} + (\Delta H/H_0)_{dip}]$ in Table II. Spectra of Mo and W clusters of a given type are strictly analogous, with the shifts of a W cluster always slightly smaller than those of its Mo counterpart. On the basis of the following observations, shifts of core terminal substituents arise mainly or exclusively from contact interactions.[39] (1) In $[Mo_2Fe_6S_8(SPh)_9]^{3-}$ [14] *o*-H, *m*-H, and *p*-H shifts alternate in sign,[40] with the shift ratios *o*-H/*m*-H (−1.56) and *p*-H/*m*-H (−1.65) being comparable to those for $[Fe_4S_4(SPh)_4]^{2-}$ (−1.35, −1.96) and $[Fe_4S_4(SPh)_4]^{3-}$ (−1.44, −1.68).[23,42] Shifts are not attenuated by distance, as would be expected from dominant dipolar (pseudocontact) interactions. (2) Shifts of methylene and methyl groups are always negative and the attenuation factors $(\Delta H/H_0)_{CH_2}/(\Delta H/H_0)_{CH_3}$ for clusters types **1**–**3** (14–17) are somewhat similar to that for $[Fe_4S_4(SEt)_4]^{2-}$ (9.3).[24] (3) Methylene resonances exhibit negative temperature coefficients of isotropic shift into the −40 to +60 °C interval (Figure 9) and roughly parallel to $\chi_M(T)$ behavior of compounds in the solid state in the same interval. Also the phenyl proton shifts in $[Mo_2Fe_7S_8(SCH_2Ph)_{12}]^{4-}$, which are negative, exhibit small but discernible shifts to higher field with increasing temperature (not shown). These observations are consistent with contact interactions effected by ligand → Fe(core) antiparallel spin transfer, affording positive (parallel) spin in S 3p-type orbitals, delocalization of which in the HOMO of the phenyl group or σ-type MO's of alkyl substituents will lead to the observed signs of the isotropic shifts.[23,24,39] Dominant contact shifts in a variety of $[Fe_4S_4(SR)_4]^{2-,3-}$ clusters have been demonstrated in some detail;[23,24,43] consequently, the related behaviors in observations 1 and 2 are of significance. Temperature coefficients of isotropic shifts in the antiferromagnetically coupled clusters $[Fe_4S_4(SR)_4]^{2-,3-}$ and in cluster types **1**–**4** are of opposite sign but are internally consistent with contact interactions inasmuch as shifts and susceptibilities *within* the two groups of compounds tend toward parallel temperature dependencies. The small range of methylene proton isotropic shifts (Table II), which are now recognized to arise mainly from contact interactions, is indicative of a high degree of electronic similarity among the Fe_3 portions of cluster types **1**–**4**.

Isotropic shifts of bridge substituents are more variant in sign and magnitude than those of terminal groups (Table II) and are suggestive of appreciable dipolar contributions. Thus alternation in the signs of all shifts is absent in $[Mo_2Fe_6S_8(SPh)_9]^{3-}$, methylene shifts of $[Mo_2Fe_6S_8(SEt)_9]^{3-}$ and $[M_2Fe_6S_9(SEt)_8]^{3-}$ are of opposite sign, and methylene and methyl or phenyl shifts in cluster types **3** and **4** are also opposite in sign. Negative methylene shifts in the latter species could arise from contact interactions since S → $Fe^{II,III}$ spin transfer is necessarily antiparallel. However, positive methyl and phenyl proton shifts (which contrast with the negative shifts of terminal CH_2CH_3 and $CH_2C_6H_5$ groups) require contribution from another mechanism. Separation of dipolar and contact contributions requires knowledge of the orientation of the molecular magnetic axis system and values of the principal susceptibilities. In the absence of such information we can only observe that the effects of (axial) susceptibility anisotropy on the shifts are expectedly larger in the bridging region, where the origin of the magnetic axis system lies and sign changes of shifts of nuclei in the same substituent are possible.[44]

C. Dynamic Behavior. A conspicuous feature of the ambient temperature spectra of the type **3** clusters $[M_2Fe_7S_8(SEt)_{12}]^{3-}$ (Figure 7) is the appearance of two signals of unequal line width and 1:1 intensity which are assigned to the methylene protons of bridging ethanethiolate groups. In apparent contrast, the type **4** clusters $[M_2Fe_7S_8(SR)_{12}]^{4-}$ (R = Et, CH_2Ph; Figure 8) exhibit one broad signal which has been similarly assigned. However, examination of the temperature dependence of the spectra of the latter species reveals that the broad signal arises as a consequence of an exchange process, as shown for $[Mo_2Fe_7S_8(SCH_2Ph)_{12}]^{4-}$ in Figure 10. At lower temperatures two signals are resolved, which coalesce at ca. 5 °C and sharpen to a single resonance at higher temperatures. Similar exchange behavior is found with $[W_2Fe_7S_8(SEt)_{12}]^{3-}$, whose signals at −9.54 and −15.8 ppm coalesce at ca. 60 °C and afford a single resonance (−10.9 ppm) at 70 °C. Coalescence of the corresponding signals of the Mo analogue was incomplete at 70 °C; partial decomposition precluded measurements at higher temperatures. It is considered probable that in cluster types **3** and **4** the source of methylene proton inequivalence and the dynamic averaging process are the same, with the activation energies for this process being different.

Potential sources of the observed methylene proton inequivalence are geometrical isomerism within the $Fe(SR)_6$ bridge unit and the intrinsic diastereotopism of these protons. Whereas in bridge fragment **5** the geminal protons of the prochiral carbon atom are

---

(39) For a discussion of experimental criteria for contact and dipolar shifts, cf. W. D. Horrocks, Jr., in "NMR of Paramagnetic Molecules", G. N. La Mar, W. D. Horrocks, Jr., and R. H. Holm, Eds., Academic Press, New York, 1973, Chapter 4.

(40) In the original report of this species certain resonances were not detected in the 90-MHz CW spectrum.[41] The complete set of terminal + bridge signals is readily observed in a 360-MHz FT spectrum, from which the assignments in Table II follow.

(41) G. Christou, C. D. Garner, and F. E. Mabbs, *Inorg. Chim. Acta*, **28**, L189 (1978).

(42) J. G. Reynolds, C. L. Coyle, and R. H. Holm, *J. Am. Chem. Soc.*, in press.

(43) G. B. Wong, D. M. Kurtz, Jr., R. H. Holm, L. E. Mortenson, and R. G. Upchurch, *J. Am. Chem. Soc.*, **101**, 3078 (1979).

(44) The dipolar shift in axial symmetry is given by $(\Delta H/H_0)_{dip} = -(\chi_\parallel - \chi_\perp)\langle(3\cos^2\theta - 1)r^{-3}\rangle$, where the symbols have their usual meaning.[39] Note that for a given molecule relative signs of shifts depend on the angle θ between the principal axis and the radius vector to the nucleus in question.

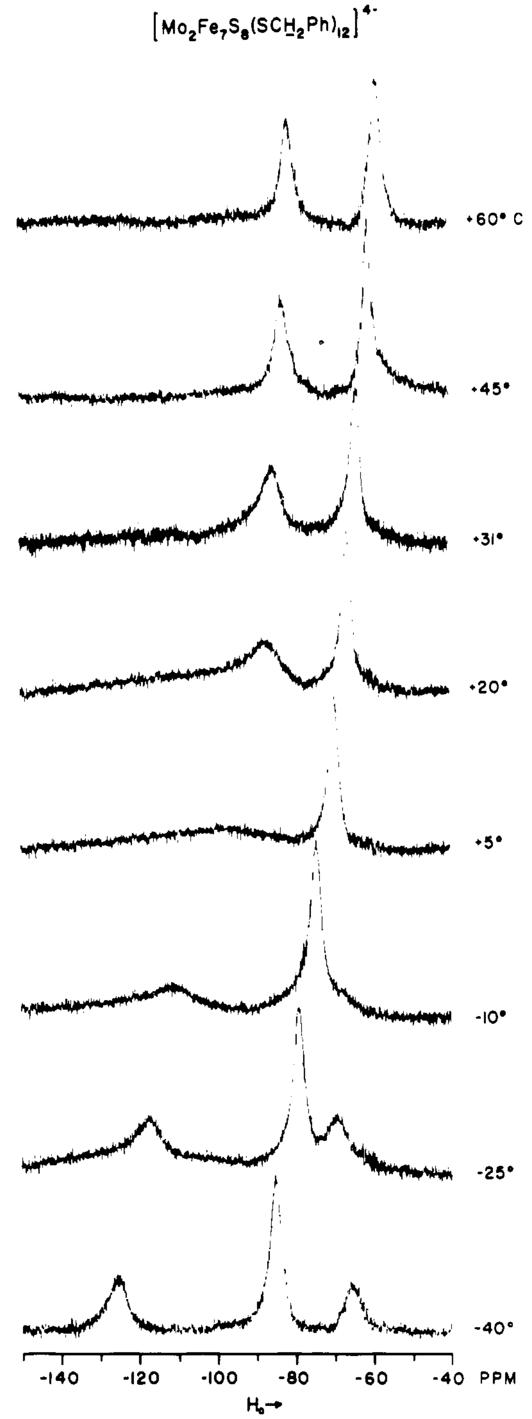

Figure 10. ^1H FT NMR spectra (100 MHz) of $(n\text{-}Bu_4N)_4[Mo_2Fe_7S_8(SCH_2Ph)_{12}]$ in CD_3CN from -40 to +60 °C illustrating the exchange averaging of bridge SCH_2 resonances. The nonexchanging resonance arises from terminal SCH_2 groups.

equivalent (isochronous) with free rotation about the S–C bond, those in fragment **6** are necessarily diastereotopic and hence

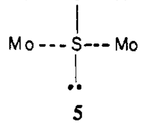

5

6

anisochronous in the absence of any process which interconverts configurations ((+), (−)) at the chiral sulfur center. The presence of a chiral center at each of the six positionally equivalent bridge sulfur atoms in cluster types **3** and **4** affords a total of eight diastereomeric molecular pairs.[45] The observation of a single sharp bridging methyl resonance at −39 to +28 °C for $[Mo_2Fe_7S_8(SMe)_{12}]^{3-}$,[46] where geminal diastereotopism is absent, is strongly suggestive of a single geometrical isomer.[45] This isomer could be **7** or **8** for only these two afford one methyl resonance

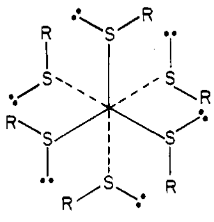

7 (+++)(−−−)

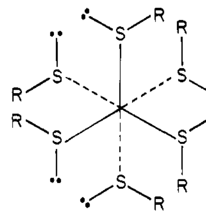

8 (+++)(+++)

each. Extrapolating this result to type **3** and **4** clusters with R = Et and CH_2Ph, we conclude that, most probably, the two bridge methylene signals are associated with one geometrical isomer rather than any mixture of isomers with incompletely resolved geminal proton shifts. This isomer is presumably the meso form **7** inasmuch as it is this form which occurs in crystalline salts of $[Mo_2Fe_7S_8(SEt)_{12}]^{3-}$ and $[M_2Fe_7S_8(SCH_2Ph)_{12}]^{4-}$.[18] In cluster types **1** and **2** only the presence of the two possible geometrical isomers can produce two bridge signals. Isomers of this sort have been detected in the ^1H NMR spectra of a series of binuclear complexes $(\eta^7\text{-}C_7H_7)Mo(\mu\text{-}SR)_3Mo(CO)_2L$,[47] but the presence of a single bridge methylene signal down to -40 °C in the spectra of $[Mo_2Fe_6S_9(SEt)_8]^{3-}$ and $[Mo_2Fe_6S_8(SEt)_9]^{3-}$ make improbable the presence of two isomers. The likely single isomer in the latter cluster is (+++)≡(−−−) for it is found in the crystalline state.[12]

There are numerous examples of inversion barriers sufficiently large to permit observation of prochiral geminal group inequivalence in organic molecules[48] and metal complexes[48,49] containing prochiral and chiral sulfur centers. Complete averaging of such inequivalence can occur by any process which inverts the configuration at a chiral sulfur center, such as that in fragment **6**. Synchronous inversion at the six sulfur centers of a single geometrical isomer could account for the observed averaging process. An alternative mechanism involves the presence of more than one conformer of a single geometrical isomer, owing to hindered rotation about $S\text{–}CH_2$ bonds, as suggested by models. Interconversion of conformers without inversion at sulfur would then account for the signal averaging, provided the intrinsic anisochrony of the methylene protons is not resolved. The latter could occur because of paramagnetic line broadening. The present information does not allow a distinction between these two possibilities. However, it is evident that activation energies are lower in the Fe^{II}-bridged clusters **4** than in the Fe^{III}-bridged clusters **3**. Thus chemical shift differences at -40 °C of ca. 70 ppm for $[Mo_2Fe_7S_8(SCH_2Ph)_{12}]^{4-}$ and of ca. 9 ppm for $[Mo_2Fe_7S_8(SEt)_{12}]^{3-}$ are averaged at ca. 5 and >70 °C, respectively. Several structural features observed in the solid state[18] may contribute to barrier differences. In $[Mo_2Fe_7S_8(SEt)_{12}]^{3-}$ the mean Fe–S bridge distance is shorter (by 0.22 Å) than in $[Mo_2Fe_7S_8$-

---

(45) One enantiomer of each pair is as follows: (+++)(+++), (++++)(++−), (+++)(+−−), (++−)(++−), (++−)(−++), (++++)(−−−), (++−)(+−−−), (+−+)(+−−−); parentheses include S atoms bonded to the same M atom.

(46) $(Et_4N)_3[Mo_2Fe_7S_8(SMe)_{12}]$ was prepared by the same method used for other $[M_2Fe_7S_8(SR)_{12}]^{3-}$ compounds, but recrystallization procedures have thus far not afforded a sample of strict analytical purity. However, secure identification has been made by Mössbauer spectroscopy (Figure 2) and electrochemistry (Figure 12). In CD_3CN solution at 28 °C terminal and bridging-group methyl protons occur as single resonances of equal intensity at -70.0 and -14.7 ppm, respectively. At -39 °C these signals shift to -87.0 and -25.8 ppm with no change in relative intensity.

(47) I. B. Benson, S. A. R. Knox, P. J. Naish, and A. J. Welch, *J. Chem. Soc., Chem. Commun.*, 878 (1978). This report details results for cases in which the R group lacks a prochiral carbon center.

(48) J. B. Lambert, *Top. Stereochem.*, **6**, 19 (1971).

(49) E. W. Abel, G. W. Farrow, K. G. Orrell, and V. Sik, *J. Chem. Soc., Dalton Trans.*, 42 (1977); E. W. Abel, A. K. Shamsuddin Ahmed, G. W. Farrow, K. G. Orrell, and V. Sik, *ibid.*, 47 (1977). These articles contain references to earlier NMR research on inversion at coordinated sulfur atoms.

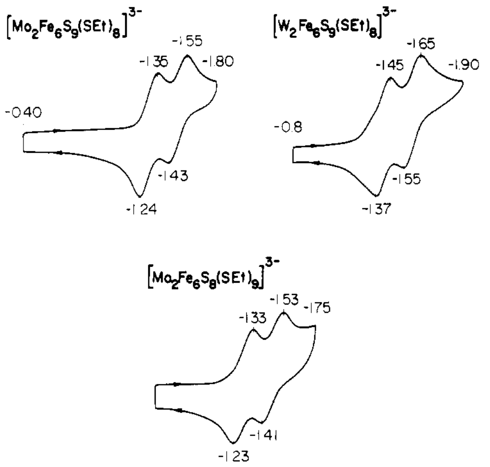

Figure 11. Cyclic voltammograms of $[M_2Fe_6S_9(SEt)_8]^{3-}$ (M = Mo, W) and $[Mo_2Fe_6S_8(SEt)_9]^{3-}$ in acetonitrile at ~25 °C at a scan rate of 100 mV/s. Peak potentials vs. SCE are indicated.

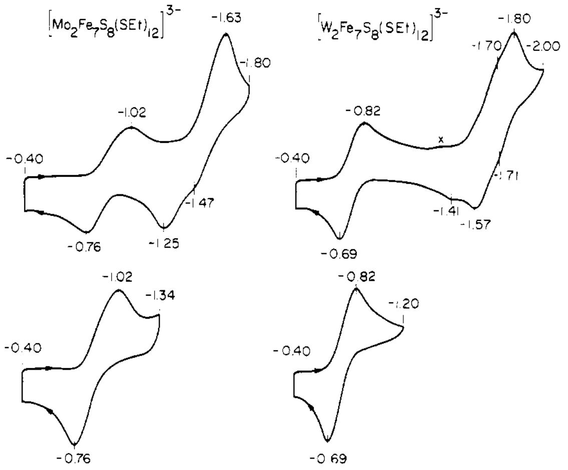

Figure 12. Cyclic voltammograms of $[M_2Fe_7S_8(SEt)_{12}]^{3-}$ (M = Mo, W) in acetonitrile at ~25 °C at a scan rate of 100 mV/s. The lower curves arise from a scan of the first redox process only. Peak potentials vs. SCE are indicated.

$(SCH_2Ph)_{12}]^{4-}$. Further, the separation between the two S_3 triangles centered on the threefold axis of the bridging unit in $[Mo_2Fe_7S_8(SCH_2Ph)_{12}]^{4-}$ is substantially larger (by 0.45 Å) than that in $[Mo_2Fe_7S_8(SEt)_{12}]^{3-}$. Consequently, the $Fe(SR)_6$ bridge region in type **4** clusters appears to be the less sterically congested, a situation that would favor a lower barrier for either inversion or bond rotation. Also the longer Fe–S bonds in these clusters suggest the possibility of a lower activation energy if they are loosened or broken in the transition state for inversion. Further discussion of these and other factors affecting relative activation energies and the mechanism of geminal proton averaging are deferred until a wider range of examples is examined.

Redox Properties. Cyclic voltammograms of cluster types **1–3** recorded under the same conditions are presented in Figures 11 and 12. No additional well-defined reductions were observed to –2.5 V; grossly irreversible oxidations at potentials more positive than –0.4 V are not considered here. Peak potential separations $|E_{p,c} - E_{p,a}| > 59$ mV indicate the absence of strict electrochemical reversibility (in some cases at scan rates up to 200 mV/s), but the value $i_{p,c}/i_{p,a} \sim 1$ for most redox events suggests effective chemical reversibility. The results in Figure 11 demonstrate the existence of the three-membered electron-transfer series 4 and

$$\underset{\mathbf{1}}{[M_2Fe_6S_9(SR)_8]^{3-}} \xrightleftharpoons{E_1} [M_2Fe_6S_9(SR)_8]^{4-} \xrightleftharpoons{E_2} [M_2Fe_6S_9(SR)_8]^{5-} \quad (4)$$

5 for types **1** and **2**, respectively. Series 5 has also been detected

$$\underset{\mathbf{2}}{[Mo_2Fe_6S_8(SR)_9]^{3-}} \xrightleftharpoons{E_1} [Mo_2Fe_6S_8(SR)_9]^{4-} \xrightleftharpoons{E_2} [Mo_2Fe_6S_8(SR)_9]^{5-} \quad (5)$$

by others for $[Mo_2Fe_6S_8(SEt)_9]^{3-}$[16b] and $[Mo_2Fe_6S_8(SPh)_9]^{3-}$.[41] Under our conditions we find for the latter cluster $E_1 = {}^1/_2(-1.03 - 0.96) = -1.00$ V and $E_2 = {}^1/_2(-1.23 - 1.13) = -1.18$ V.[50] Reductions of $[W_2Fe_6S_8(SEt)_9]^{3-}$ are reported to be irreversible.[16b] Voltammetry of the type **3** clusters $[M_2Fe_7S_8(SEt)_{12}]^{3-}$ in Figure 12 reveals an initial reduction (E_1) well separated from further reductions, two of which are just resolvable with M = W ($E_{2p,c} = -1.70$ V, $E_{3p,c} = -1.80$ V). For the Mo complex a single feature is observed at $E_{p,c} = -1.63$ V, which is presumably a composite inasmuch as two reductions ($E_{2p,c} = -1.67$ V, $E_{3p,c} = -1.72$ V) are discernible in voltammograms of DMF solutions. These findings lead to formulation of the four-membered series 6 for type **3** clusters.

$$\underset{\mathbf{3}}{[M_2Fe_7S_8(SR)_{12}]^{3-}} \xrightleftharpoons{E_1} \underset{\mathbf{4}}{[M_2Fe_7S_8(SR)_{12}]^{4-}} \xrightleftharpoons{E_2} [M_2Fe_7S_8(SR)_{12}]^{5-} \xrightleftharpoons{E_3} [M_2Fe_7S_8(SR)_{12}]^{6-} \quad (6)$$

Cluster types **1–4** present an interesting case of two structurally indistinguishable redox sites ($MFe_3S_4(SR)_3$ clusters) separated by distances which vary according to bridge structure. The two processes in series 4 and 5 are assigned to stepwise reduction of the two individual clusters, $(Ox\text{–}Ox)^{3-} \rightleftharpoons (Ox\text{–}Red)^{4-} \rightleftharpoons (Red\text{–}Red)^{5-}$. The equilibrium comproportion constant for reaction 7 is given by eq 8.[51,52] If the sites are noninteracting, $K_{com} = 4$,

$$(Ox\text{–}Ox)^{3-} + (Red\text{–}Red)^{5-} \rightleftharpoons 2(Ox\text{–}Red)^{4-} \quad (7)$$

$$E_1 - E_2 = 0.0591 \log K_{com} \quad (8)$$

the statistical value, and $E_1 - E_2 = 36$ mV. From the peak potentials in Figure 11, $E_1 - E_2 = 0.19$ V (~4.4 kcal/mol) and $K_{com} \simeq 1.6 \times 10^3$ for the three clusters, indicating a small influence of one site on the other during the course of reduction. The constant potential difference signifies that the variation of site separation based on Mo···Mo distances[12] (3.19 and 3.31 Å in **1**; 3.67 Å in **2**) is insufficient to alter interaction energies between the sites.

Identification of the initial reduction product in series 6 follows from direct synthesis of three examples of cluster type **4**. Although the first reduction process, even when scanned separately, is not strictly reversible by cyclic voltammetric criteria, it is chemically reversible, as shown by both chemical and electrochemical oxidation of type **4** to type **3** clusters. Oxidation of $[W_2Fe_7S_8(SEt)_{12}]^{4-}$ occurs at a potential E_1 which conforms to that obtained from peak potentials in Figure 12. Consequently, the first step in the series is the bridge $Fe^{III} \rightarrow Fe^{II}$ reduction, whose potential exhibits a dependence on cluster atom M = Mo ($E_1 = -0.89$ V) or W ($E_1 = -0.76$ V). Further reductions (E_2, E_3) are assigned to individual cluster sites and occur at more negative potentials than E_1 and E_2 for types **1** and **2**. Consistent with this assignment are small $E_2 - E_3$ values, as would be anticipated from the large M···M distances in $[M_2Fe_7S_8(SR)_{12}]^{3-,4-}$[18] (6.64–6.94 Å). With $[W_2Fe_7S_8(SEt)_{12}]^{3-}$, for example, $E_2 - E_3 \simeq 0.10$ V (~2.3 kcal/mol) and $K_{com} \simeq 50$. Among cluster species this situation represents an approach to the redox properties of clostridial-type ferredoxins, which contain two nearly identical Fe_4S_4 redox sites. Eisenstein and Wang[53] first recognized the statistical 36-mV potential difference between the sites. Subsequent measurements have shown that $E_1 - E_2 \lesssim 10\text{–}15$ mV,[54] smaller than $E_2 - E_3$

---

(50) Owing to the lack of electrochemical reversibility, the potentials $E = {}^1/_2(E_{p,c} + E_{p,a})$ quoted here and elsewhere are approximate values of, rather than true, formal potentials.

(51) J. B. Flanagan, S. Margel, A. J. Bard, and F. C. Anson, *J. Am. Chem. Soc.*, **100**, 4248 (1978).

(52) R. R. Gagné, C. A. Koval, T. J. Smith, and M. C. Cimolino, *J. Am. Chem. Soc.*, **101**, 4571 (1979).

(53) K. K. Eisenstein and J. H. Wang, *J. Biol. Chem.*, **244**, 1720 (1969).

values in series 6 presumably because of the substantially larger intersite distance of $\lesssim 12$ Å.[55]

Summary

At this point we summarize the principal results and conclusions from the present and prior investigations of Mo–Fe–S clusters in this laboratory.[11-13,18]

(i) Reaction system 1 affords four principal cluster products: $[M_2Fe_6S_9(SR)_8]^{3-}$ (**1**), $[Mo_2Fe_6S_8(SR)_9]^{3-}$ (**2**), $[M_2Fe_7S_8(SR)_{12}]^{3-}$ (**3**), and $[M_2Fe_7S_8(SR)_{12}]^{4-}$ (**4**); relative product yields are dependent upon the choice of the R substituent, quaternary ammonium countercation, and reaction conditions. (From a similar reaction system, cluster type **2** with M = Mo[14-16a] and W[16b] can be isolated.)

(ii) All products in i possess an overall "double-cubane" structure in which individual $MFe_3S_4(SR)_3$ clusters are linked through atoms M by different bridge units. Within each species and among all species, MFe_3S_4 cores are exactly or virtually isodimensional. On the basis of Shannon–Prewitt radii[56] it is unlikely that this relationship would exist if M oxidation states differed by more than one unit.

(iii) Isotropic ^{1}H shifts of terminal Fe–SR substituents arise from dominant contact interactions associated with RS → Fe(core) antiparallel spin delocalization, whereas the shifts of M–(SR)–M and M–(SR)–Fe substituents cannot be explained similarly and thus contain significant dipolar contributions.

(iv) One geometrical isomer, presumably **7**, is present in solutions of cluster types **3** and **4**. Pairs of ^{1}H signals from geminal protons attached to prochiral bridge carbon atoms in these clusters could arise from their intrinsic diastereotopism or the presence of conformers, owing to restricted $S–CH_2$ bond rotation. Chemical shift anisochrony of these protons is accentuated by isotropic interactions. Cluster types **1** and **2** also appear to exist as single isomers in solution.

(v) Cluster types **1** and **2** form the three-membered electron-transfer series 4 and 5, respectively, in which stepwise reduction is associated with individual clusters ($E_1 - E_2 \simeq 0.19$ V). Cluster type **3** exhibits the four-membered series 6 in which the initial step is bridge Fe^{III}/Fe^{II} reduction and the two remaining steps are cluster reductions ($E_2 - E_3 \lesssim 0.10$ V). Cluster redox processes are weakly coupled, with potential differences in series 6 more closely approaching the statistical value, owing to much larger intercluster distances.

(vi) On the basis of the following collective experimental evidence, the Fe_3 core portions within and among all cluster types **1–4** are virtually equivalent electronically: (a) isomer shifts at 77 K fall in a narrow range whose limits (0.27–0.33 mm/s) additionally indicate substantial electronic delocalization over the Fe sites, which, however, are themselves not precisely equivalent; (b) hyperfine magnetic fields at the more or less intense Fe subsites are very similar; (c) from the small interval (−51 to −55 ppm) of terminal $Fe–SCH_2CH_3$ isotropic shifts, contact interactions are of comparable magnitude; (d) redox potentials of series 4 (M = Mo) and 5 are nearly identical; in series 4 and 6 potentials show a $\lesssim 0.10$-V dependence on M in cluster reductions.

(vii) Isomer shifts and Fe–S bond distance trends[12,18] collectively favor the mean oxidation state description $Fe^{2.67+}$ ($4Fe^{III} + 2Fe^{II}$) for core atoms in a given cluster type and require that the M atom oxidation state sum be +7 in **1** and +6 in **2–4**. Together with structural feature ii, these observations lead to the core formal electronic descriptions **9** and **10**, in which Fe_3 portions of individual

$$\underset{\mathbf{9}}{[Mo^{4+}Fe^{3+}{}_2Fe^{2+}S_4]^{4+}} + \underset{\mathbf{10}}{[Mo^{3+}Fe^{3+}{}_2Fe^{2+}S_4]^{3+}} \qquad (\text{type } \mathbf{1})$$

$$2\underset{\mathbf{10}}{[Mo^{3+}Fe^{3+}{}_2Fe^{2+}S_4]^{3+}} \qquad (\text{types } \mathbf{2–4})$$

cores are electronically equivalent.[57] While such descriptions are obviously formalisms, especially in cases of electron delocalization, they do serve to define (or limit) individual core oxidation levels and provide a starting point for development of a more satisfactory electronic structural description.

The results in vi and vii are particularly interesting for they reveal that the same mean Fe oxidation state is stabilized in all clusters which spontaneously self-assemble in reaction system 1; indeed, with the exception of type **1**, cores within a given cluster type are isoelectronic. This situation is similar to that encountered in other systems where only $[Fe_4S_4(SR)_4]^{2-}$ clusters are formed in the presence of sufficient thiolate reductant.[59,60] In a redox sense the latter buffers the assembled cluster in a fixed oxidation level.[61] The view which emerges from ii–vii is that of weakly coupled, nearly or exactly equivalent MFe_3S_4 cores in cluster types **1–4** with primary structural and electronic differences associated with the bridge units (including atoms M). Further experimentation directed toward the synthesis of reduced clusters and examination of their electronic properties, as well as reactivity properties of cluster types **1–4**, is under way.

Acknowledgments. This research was supported by NSF Grant CHE77-04397 at Stanford University and by the National Science Foundation at the Francis Bitter National Magnet Laboratory. We thank T. D.-Y. Chung, R. E. Palermo, Dr. C. L. Coyle, and J. G. Reynolds for experimental assistance and Professor D. Coucouvanis for access to results prior to publication.

---

(54) E. L. Packer, H. Sternlicht, E. T. Lode, and J. C. Rabinowitz, *J. Biol. Chem.*, **250**, 2062 (1975).

(55) E. T. Adman, L. C. Sieker, and L. H. Jensen, *J. Biol. Chem.*, **248**, 3987 (1973); **251**, 3801 (1976).

(56) R. D. Shannon and C. T. Prewitt, *Acta Crystallogr., Sect. B*, **25**, 925 (1969); R. D. Shannon, *Acta Crystallogr., Sect. A*, **32**, 751 (1976).

(57) If the description $Fe^{2.5+}$ ($3Fe^{III} + 3Fe^{II}$) is entertained, no formulation can be written for any cluster type **1–4** in which individual cores are electronically equivalent. Given that the core structural relationship in ii has been found in 11 compounds to date[11-18] and that $[Fe_4S_4(SR)_4]^{2-,3-}$ clusters exhibit core structural differences,[26,58] it seems improbable that core structural inequivalence associated with electronic inequivalence would not have been detected. With this description *both* the sums of Fe oxidation states and M oxidation states must differ by at least one unit in types **2–4** (e.g., $[M^{4+}Fe^{3+}Fe_2{}^{2+}S_4]^{3+} + [M^{3+}Fe_2{}^{3+}Fe^{2+}S_4]^{3+}$ in the most favorable case). Apparent core structural equivalence in two salts of $[Mo_2Fe_6S_9(SEt)_8]^{3-}$[12] (in one case not crystallographically imposed) is not necessarily inconsistent with the description **9–10**. Six-coordinated $Mo^{III}–Mo^{IV}$ radii differ by ~0.04 Å[56] and thus could allow disordered packing, a situation not uncommon in mixed-valence compounds.

(58) J. M. Berg, K. O. Hodgson, and R. H. Holm, *J. Am. Chem. Soc.*, **101**, 4586 (1979).

(59) B. A. Averill, T. Herskovitz, R. H. Holm, and J. A. Ibers, *J. Am. Chem. Soc.*, **95**, 3523 (1973).

(60) G. Christou and C. D. Garner, *J. Chem. Soc., Dalton Trans.*, 1093 (1979).

(61) Cluster types **1–4** display similarities in core structure, absorption spectra, Mössbauer parameters, and dependence of redox potential on R substituent with $[Fe_4S_4(SR)_4]^{2-}$ species. However, these similarities must be viewed as somewhat fortuitous in that any reasonable assignment of core oxidation levels (e.g., **9** and **10**) does not permit an isoelectronic relation with the 54 e$^-$ $[Fe_4S_4]^{2+}$ core of $[Fe_4S_4(SR)_4]^{2-}$.